Biochimica et Biophysica Acta, 764 (1984) 46–54
Elsevier

BBA 41424

KINETICS AND THERMODYNAMICS OF THE $P870^+Q_A^-$ → $P870^+Q_B^-$ REACTION IN ISOLATED REACTION CENTERS FROM THE PHOTOSYNTHETIC BACTERIUM *RHODOPSEUDOMONAS SPHAEROIDES*

L.J. MANCINO, DAVID P. DEAN and ROBERT E. BLANKENSHIP *

Department of Chemistry, Amherst College, Amherst, MA 01002 (U.S.A.)

(Received July 19th, 1983)

Key words: Bacterial photosynthesis; Electron transfer; Reaction center; Quinone; Free energy; (Rps. sphaeroides)

The temperature dependences of the $P870^+Q_A^-$ → $P870Q_A$ and $P870^+Q_B^-$ → $P870Q_B$ recombination reactions were measured in reaction centers from *Rhodopseudomonas sphaeroides*. The data indicate that the $P870^+Q_B^-$ state decays by thermal repopulation of the $P870^+Q_A^-$ state, followed by recombination. $\Delta G°$ for the $P870^+Q_A^-$ → $P870^+Q_B^-$ reaction is -6.89 kJ · mol^{-1}, while $\Delta H° = -14.45$ kJ · mol^{-1} and $-T\Delta S° = +7.53$ kJ · mol^{-1}. The activation ethalpy, $H^‡$, for the $P870^+Q_A^-$ → $P870^+Q_B^-$ reaction is $+56.9$ kJ · mol^{-1}, while the activation entropy is near zero. The results permit an estimate of the shape of the potential energy curve for the $P870^+Q_A^-$ → $P870^+Q_B^-$ electron transfer reaction.

Introduction

Reaction centers of photosynthetic bacteria are pigment protein complexes that efficiently convert photon energy into redox energy. In purple photosynthetic bacteria, the complex contains four bacteriochlorophyll molecules, two bacteriopheophytin molecules, two quinones, an iron atom and three peptides [1,2]. The primary electron transfer event occurs from excited bacteriochlorophyll(s) that in the ground state absorb maximally at 870 nm (P870). The initial electron acceptor is either a bacteriochlorophyll (B) or a bacteriochlorophyll-bacteriopheophytin complex (I) [3]. The charge-separated state $P870^+I^-$ is stabilized against recombination by a rapid ($\tau = 200$ ps) electron transfer [4,5] to a quinone acceptor (Q_A), which in *Rhodopseudomonas sphaeroides* is ubiquinone [6].

A second quinone acceptor is reduced in 200 μs, leading to the state $P870^+Q_B^-$. The $Q_A^-Q_B$ → $Q_AQ_B^-$ reaction can be measured by a double-flash technique [7,8], a kinetic analysis of the recombination [9], or most easily by monitoring the absorbance of bacteriopheophytin in the near infrared (750 nm), which exhibits somewhat different electrochromic shifts when Q_A or Q_B is reduced [10]. The activation energy for this reaction (in chromatophores of *Chromatium vinosum, Rps. sphaeroides* and *Rhodospirillum rubrum*) has been determined to be between 8.3 and 10.5 kcal · mol^{-1} [7,9,11].

The second quinone acceptor can accept two electrons, and the semiquinone form is stable for many minutes. This gives rise to binary oscillations in semiquinone content if an efficient electron donor is present to rereduce $P870^+$ before recombination can take place [12,13]. The system exhibits a complex pH dependence, in which oscillations in proton uptake that are out of phase with semiquinone formation are observed at low pH. The strength of oscillation in proton uptake is attenuated in the neutral region and eventually disappears at high pH [14]. The rate of the $Q_A^-Q_B$

* To whom correspondence should be addressed.

$\rightarrow Q_A Q_B^-$ reaction is only weakly pH-dependent 0.3 decade/pH unit), indicating that proton uptake is not rate-limiting for this reaction [14,11,15]. However, the rate of the $Q_A^- Q_B^- \rightarrow Q_A Q_B^{2-}$ reaction is strongly pH-dependent [11,14,15] (1 decade/pH unit); the product of this reaction is the fully reduced quinol $Q_B H_2$, which then dissociates from the reaction center and is replaced by an oxidized quinone.

If reaction centers contain only a single quinone and no electron donors, or if the inhibitor *o*-phenanthroline is present, the state $P870^+ Q_A^-$ is formed after a flash and decays by electron recombination with τ approx. 100 ms at room temperature [16]. If the reaction center contains two quinones, the state $P870^+ Q_B^-$ is formed after a flash and decays with τ approx. 1 s at room temperature [16,17]. Reaction centers with average quinone contents between one and two exhibit biphasic kinetics; the amplitude of the 1 s phase is linearly related to the quinone content above one [17]. Thus the 100 ms phase reflects recombination from the $P870^+ Q_A^-$ state in reaction centers without a functional Q_B, while the 1 s phase reflects recombination from the $P870^+ Q_B^-$ state.

The mechanism of the $P870^+ Q_B^- \rightarrow P870 Q_B$ recombination has been the subject of considerable discussion. The question has been whether the recombination between $P870^+$ and Q_B^- is direct or whether it proceeds via thermal repopulation of Q_A^-, followed by recombination from the state $P870^+ Q_A^-$. Stopped-flow experiments in which *o*-phenanthroline was mixed with reaction centers preilluminated so as to form the state $P870^+ Q_B^-$ implied that the recombination was direct, although an ambiguity existed if *o*-phenanthroline was unable to bind in the state $P870^+ Q_B^-$ [17]. Subsequently, it was shown that indeed *o*-phenanthroline is ineffective in this state [18,19] and that the indirect pathway alone can account for the decay of $P870^+ Q_B^-$ [14,19,8].

The free-energy gap between $P870^+ Q_A^-$ and $P870^+ Q_B^-$ has been measured by redox titrations [20,21], delayed fluorescence [22], double-flash techniques [8] and by analyzing the decay of the $P870^+ Q_B^-$ state [14,19,8]. All the methods give remarkably consistent values of -60 to -80 meV *, equivalent to an equilibrium constant of 10–20. Kleinfeld et al. [8] determined the standard enthalpy and entropy contributions to the free-energy storage to be -230 and -0.55 meV/K, respectively. We have also determined the free energy, enthalpy and entropy of this reaction with similar but not identical results. Additionally, we have determined activation parameters for this reaction. Together, the results allow an estimate of the shape of the potential energy curve for the $P870^+ Q_A^- \rightarrow P870^+ Q_B^-$ reaction.

Materials and Methods

Reaction center isolation. Cells (approx. 200 g) of *Rps. sphaeroides* R-26 were suspended in 20 mM Tris buffer, pH 7.5, 100 mM NaCl/5 mM $MgCl_2$ a small amount of DNAase was added, and the solution was passed three times through a French pressure cell at 20000 $lb \cdot inch^{-2}$. After a 15 min centrifugation at $8000 \times g$ to remove unbroken cells, the chromatophores were pelleted by a 1 h, $300000 \times g$ centrifugation (50000 rpm, Beckman Ti 50.2 rotor). The chromatophores were resuspended in 20 mM Tris, pH 7.5, 100 mM NaCl, adjusted to A = 50 at 870 nm, and lauryl dimethyl amine oxide (LDAO, gift of Onyx Chemical Co., Jersey City, NJ) was added to a final concentration of 0.45%. Centrifugation at $300000 \times g$ for 1 h yielded a chromatophore pellet and a supernatant that contained cytochrome c_2 but was largely devoid of reaction centers. A second detergent treatment of the resuspended pellet by 0.4% LDAO followed by a 1 h, $300000 \times g$ centrifugation solubilized the reaction centers. The supernatant from this second detergent treatment was carefully drawn off the pellet, and dialyzed vs. 10 mM Tris, pH 8.0, 0.1% LDAO/10 μM EDTA (Tris/LDAO buffer, which is called 'buffer 1' hereafter). For final purification, the crude reaction centers were loaded onto a 3×50 cm DEAE-Sephacel (Pharmacia) column previously equilibrated with buffer 1, washed with 300 ml buffer 1/100 mM NaCl, and eluted using a 100–400 mm NaCl gradient in the same buffer. The purest

* The convention that spontaneous reactions have negative free energy changes will be used throughout this paper, instead of the opposite convention usually used with electrochemical measurements.

fractions were pooled, dialyzed vs. buffer 1 and rechromatographed. The final yield was an A_{800} · vol (ml) of approx. 150, with an A_{280}/A_{800} ratio of 1.3.

For the variable temperature experiments in this paper, the reaction centers were dialyzed into 10 mM pyrophosphate buffer (pH 8.0)/0.1% LDAO. Pyrophosphate has an extremely low temperature coefficient of pK_a [23]; pH changes coupled to temperature changes are minimized with this buffer.

Ubiquinone-50 (Sigma) was added to samples of reaction centers from a 2 mM stock solution in ethanol to give a 20 : 1 molar ratio of quinone to reaction center. After overnight incubation, the reconstituted reaction centers were clarified by passage through a 0.2 μm membrane filter (Gelman, Ann Arbor, MI) and diluted to a final reaction center concentration of 0.6–1.4 μM.

Kinetic measurements. Laser-induced absorption changes were measured in the home-built single-beam spectrophotometer previously described [24]. The 583.5 nm 1 μs pulses (attenuated to approx. 100 mJ using neutral density filters) were of saturating intensity. A silicon photodiode (UDT 455) served as detector for the recombination experiments, all of which were carried out with 865 nm measuring light of 6 nm bandpass. The intensity of the measuring beam was attenuated using calibrated neutral density filters. Four traces of both 1 and 5 s sweep were averaged at each set of conditions. A photomultiplier (Hamamatsu R928) was used for the measurements of the $P870^+Q_A^-$ $\rightarrow P870^+Q_B^-$ reaction, carried out with 750 nm measuring light of 6 nm bandpass. Ten traces of 2–10 ms sweep were averaged at each set of conditions.

All experiments were carried out using a water-jacketed fluorescence cuvette. The temperature was controlled using a refrigerated bath and measured with a Cu-constantan thermocouple immersed directly into the sample.

Data analysis. The recombination data were transferred to a Digital Equipment VAX 11/780 computer for analysis. Traces were converted from transmittance to absorbance, and fit to an equation of the form $\Delta A(t) = A \exp(-k_f t) + B \exp(-k_s t)$, where A and B are preexponential factors and k_f and k_s are fast and slow decay constants. The nonlinear least-squares fit was performed using the CURFIT routine described by Bevington [25]. Derivatives were calculated analytically. In some cases, the slow decay constant was obtained using only the latter part of the 5 s-traces, when the fast decay contribution was insignificant. For these determinations, a Hewlett Packard 9825B computer was used to perform a weighted linear least-squares fit to ln ΔA vs. time. The slow decay constants determined using this method were within 4% of the values obtained using the nonlinear double exponential program. In all cases, the fast decay constants were determined from the 1 s sweeps using the nonlinear fitting method.

The 750 nm bandshift data were fit using a weighted linear least-squares fit to ln ΔA vs time. The infinity-time value was obtained by averaging data in the latter portion of the sweep, after the decay was complete (see Fig. 1b).

The linear least-squares fits to the data of Figs. 3 and 4 were determined using standard analysis techniques; the quoted errors are 95% confidence values [26].

Results

Typical data traces for recombination, measured at 865 nm, and the $P_{870}^+Q_A^-Q_B \rightarrow P_{870}^+Q_AQ_B^-$ reaction, measured at 750 nm, are shown in Fig. 1. For the recombination experiments, the quinone content of the sample was adjusted so as to give approximately equal amplitudes of fast (approx. 100 ms) and slow (approx. 1 s) decay. This afforded a simultaneous measurement of both the rate constants k_f and k_s on a single sample.

The k_s values were found to be sensitive to the identity of the measuring light, with higher intensities producing larger values of k_s (Fig. 2). Analysis of a kinetic scheme appropriate to this system (see Appendix) predicts the linear relation observed between k_s and the intensity of the measuring light. The relationship between the observed rate constant, k_s, and the intrinsic constants of the system is:

$$k_s = k_{12} + \frac{k_{21}}{K+1} + \frac{k_{31}K}{K+1} \quad (1)$$

where k_{12} is the rate constant for transitions in-

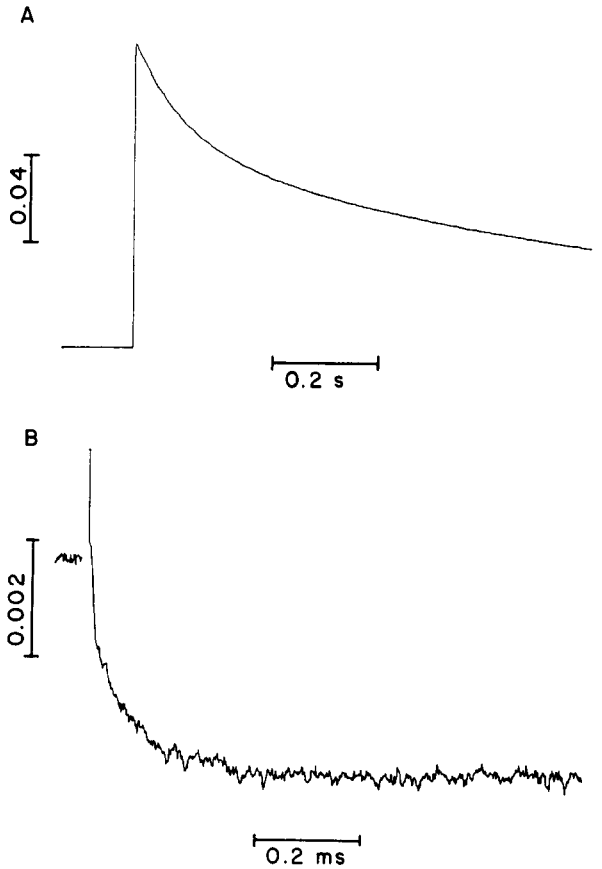

Fig. 1. Laser-flash-induced transmittance changes in reaction centers from *Rps. sphaeroides* R-26. (A) Bleaching of P870 measured at 865 nm as described in Materials and Methods; (B) bacteriopheophytin bandshift measured at 750 nm. In both curves an upward deflection is an absorbance decrease.

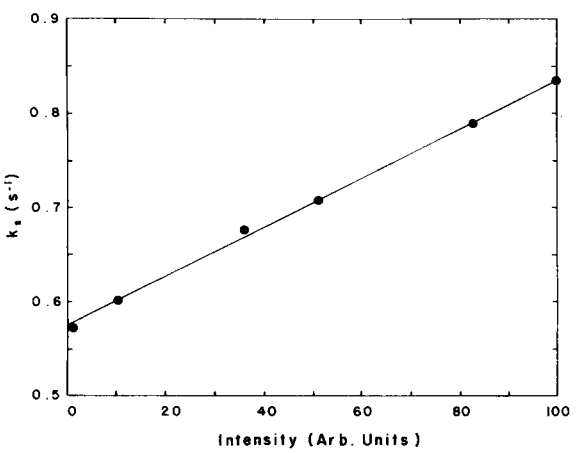

Fig. 2. The measuring light intensity dependence of the slow decay constant for recombination, measured at 865 nm.

duced by the measuring light, k_{21} and k_{31} are the rate constants for direct recombination from the states $P870^+Q_A^-$ and $P870^+Q_B^-$, respectively, and K is the equilibrium constant of the $P870^+Q_A^- \rightarrow P870^+Q_B^-$ reaction (see Appendix). Previous work (see Introduction) has shown that the direct recombination process is unimportant in the decay of the $P870^+Q_B^-$ state, indicating that the last term in Eqn. 1 is negligible. At zero intensity of measuring light, $k_f = k_{21}$, the first term in Eqn. 1 is zero, and K is given by Eqn. 2:

$$K = \frac{k_f^0}{k_s^0} - 1 \tag{2}$$

where the superscript refers to the value of k_f or k_s extrapolated to a measuring light intensity of zero.

Equilibrium constants were determined using Eqn. 2 at temperatures ranging from 273 to 303 K. A Van 't Hoff plot (ln K vs $1/T$) yields a standard state enthalpy change of -14.45 ± 1.1 kJ · mol^{-1} (-150 ± 11 meV) (Fig. 3). The entropic contribution (determined from the intercept of the Van 't Hoff plot) at 293 K is $-T\Delta S^0 = +7.53 \pm 0.9$ kJ · mol^{-1} ($+78 \pm 9$ meV). The free-energy change is -6.89 ± 0.13 kJ · mol^{-1} (-71.4 ± 1.4 meV), determined from the K value at 293 K (16.9 ± 0.9).

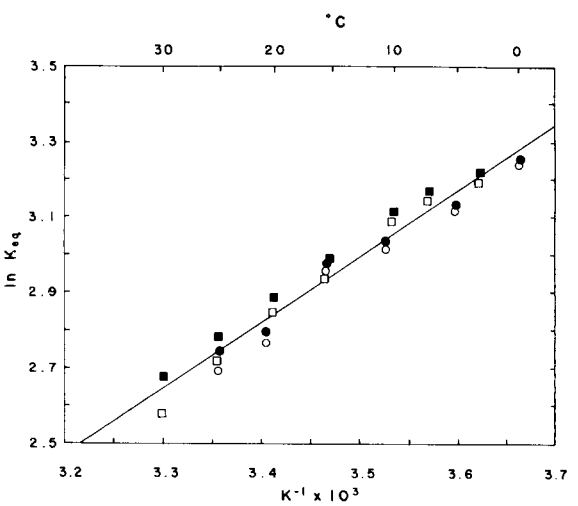

Fig. 3. Van 't Hoff plot of equilibrium constants determined using Eqn. 2. Open symbols, nonlinear least-squares analysis of both k_f and k_s; filled symbols, nonlinear analysis of k_f, linear semilog analysis of k_s, as described in Materials and Methods. Circles and boxes are two separate sets of data acquired on different days.

The results are summarized in Table I, along with similar values from the literature.

A series of measurements of the 750 nm bandshift were carried out in order to determine the activation parameters for the $P870^+Q_A^- \rightarrow P870^+Q_B^-$ reaction. Since the process that is measured is the approach to equilibrium (actually pseudoequilibrium), the measured rate constant is actually the sum of the forward and reverse rate constants (see Appendix). Values for the forward and reverse rate constants at each temperature were obtained from the measured values of k and the equilibrium constant at that temperature.

The analysis of the kinetic data is carried out within the context of the activated complex theory for reaction rates [28]. The rate constant is related to thermodynamic parameters of the transition state by Eqn. 3:

$$k = \kappa \frac{kT}{h} \exp\left(-\frac{\Delta S^{\ddagger}}{R}\right) exp\left(-\frac{\Delta H^{\ddagger}}{RT}\right) \qquad (3)$$

where κ is a transmission coefficient (usually assumed to have a value of 1), k and h are Boltzmann's and Planck's constants, respectively, and $\Delta S^{\ddagger}$ and $\Delta H^{\ddagger}$ are entropy and enthalpy changes associated with formation of the transition state.

Arrhenius ($\ln k$ vs $1/T$) and Eyring ($\ln (k/T)$ vs. $1/T$) plots of the forward rate constant k_{23} are shown in Fig. 4. The activation enthalpy is obtained directly from the slope of an Eyring plot, yielding $\Delta H^{\ddagger} = +56.9 \pm 4.6$ kJ · mol^{-1} ($+590 \pm 41$ meV). The Arrhenius plot yields an identical value of $\Delta H^{\ddagger}$ using the relation $E_a = \Delta H^{\ddagger} + RT$ appropriate for solution reactions [27]. The raw data (uncorrected for the reverse reaction) yield an apparent activation energy of $E_a = 60.0$ kJ · mol^{-1} (14.3 kcal · mol^{-1}).

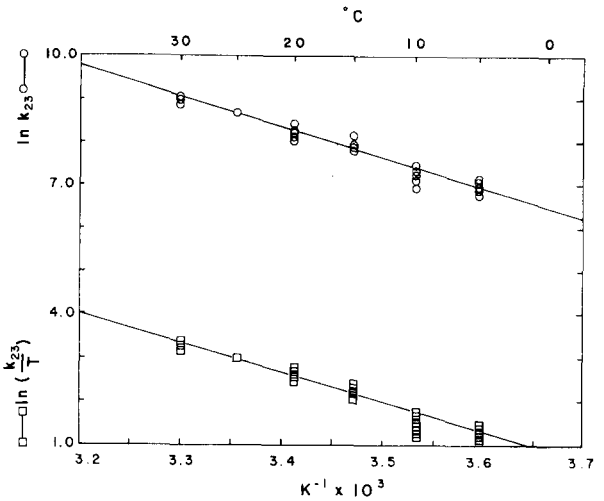

Fig. 4. Arrhenius ($\ln k_{23}$) (○———○) and Eyring ($\ln(k_{23}/T)$) (□———□) plots of the rate constant k_{23} for the $P870^+Q_A^-Q_B \rightarrow P870^+Q_AQ_B^-$ reaction, measured at 750 nm (Fig. 1B). The apparent rate constants were corrected for the reverse reaction as described in the text.

The intercept of the Eyring plot yields the activation entropy. At 298 K, $-T\Delta S^{\ddagger} = -5.4 \pm 5$ kJ · mol^{-1} (-56 ± 52 meV). The activation free energy determined from the rate constant at 298 K is $\Delta G^{\ddagger} = +51.6 \pm 0.3$ kJ · mol^{-1} ($+534 \pm 3$ meV).

The magnitude (ΔA) and rate constant (k_{23}) of the 750 nm absorption change that reflects the $Q_A^-Q_B \rightarrow Q_AQ_B^-$ reaction was monitored as a function of added ubiquinone (data not shown). The magnitude of the 750 nm absorbance change doubled upon addition of a 10-fold molar excess of ubiquinone to reaction centers, and then re-

TABLE I

Units are kJ · mol^{-1}, except for values in parentheses which are meV.

ΔG^0		ΔH^0		$-T\Delta S^0$		Reference
-6.89 ± 0.13	(-71.4 ± 1.4)	-14.45 ± 1.1	(-150 ± 11)	$+7.53 \pm 0.9$	($+78 \pm 9$)	This work
	(-68)		(-230)		($+161$)	Ref. 8
	(-70 ± 10)	–		–		Ref. 14
	(-78 ± 8)	–		–		Ref. 22
$\Delta G^{\ddagger}$		$\Delta H^{\ddagger}$		$-T\Delta S^{\ddagger}$		Reference
$+51.6 \pm 0.3$	($+534 \pm 3$)	$+56.9 \pm 4.6$	($+590 \pm 41$)	-5.4 ± 5	(-56 ± 52)	This work

mained constant to a 50-fold excess. The rate constant k_{23} was unchanged throughout the entire range of quinone concentrations. This establishes that the residence time of Q_B on the reaction center is long relative to the millisecond time-scale of these experiments, and that the reaction is properly considered as a true first-order process rather than second-order or pseudo-first-order.

Discussion

The thermodynamic parameters determined in this study are shown schematically in Fig. 5. Under our conditions, the $P870^+Q_A^-Q_B \rightarrow P870^+Q_AQ_B^-$ reaction has a large positive activation enthalpy and a negative overall enthalpy change, partially offset by a negative overall entropy change. The activation entropy is near zero, consistent with the unimolecular nature of this reaction [27]. The activation energy determined from the Arrhenius plot of the 750 nm bandshift data uncorrected for the reverse reaction is somewhat higher than values previously found for this reaction (14.3 kcal · mol^{-1} vs 8.3–10.5 kcal · mol^{-1}) [7,9,11]. Previous measurements have all been carried out in chromatophores, while ours utilized isolated reaction centers. Vermeglio [11] found that the apparent rate constant for the $Q_A^-Q_B \rightarrow Q_AQ_B^-$ reaction was 3–5 fold faster in chromatophores of *Rps. sphaeroides* than in isolated reaction centers. Minor changes in reaction-center geometry induced by the isolation procedure are probably responsible for these differences.

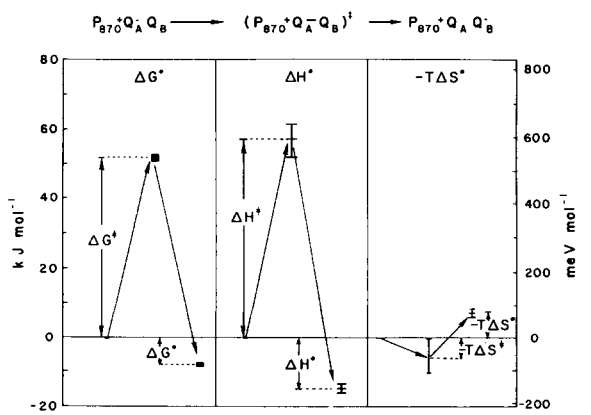

Fig. 5. Thermodynamic parameters of the $P870^+Q_A^-Q_B \rightarrow P870^+Q_AQ_B^-$ reaction, taken from Table I.

The $Q_A^-Q_B \rightarrow Q_AQ_B^-$ reaction is clearly not second order with respect to quinone (see Results). The situation with respect to H^+ is somewhat less clear. The apparent first-order rate constant for this reaction does show a pH effect [14,11], but the reaction is only weakly pH-dependent (0.3 decade/pH unit), implying that it is not a true bimolecular process. The absorption spectra of both Q_A^- and Q_B^- are most consistent with the anionic semiquinone [12,13], although a proton bound to a nearby protein group as suggested by Wraight [14] could possibly be (but apparently is not) an essential accompanying event (e.g., rate determining) to this electron transfer. Wraight has found that protons are taken up on the first flash at neutral to alkaline pH (but not at acid pH) and that the apparent rate constant for proton uptake is slightly slower than the rate of electron transfer [14]. We have therefore analyzed our data in terms of a unimolecular reaction, with the realization that the pH behavior is complex. However, the only thermodynamic parameter affected by this choice is the activation entropy.

The second electron to reduce Q_B is clearly accompanied by rate-determining proton binding [14,11]. This is presumably because the dianion of the quinone has a very negative redox potential, and must be stabilized by a positive charge [14,15].

The overall free-energy change found for the $Q_A^-Q_B \rightarrow Q_AQ_B^-$ reaction is quite close to values found previously using a variety of methods [8,14,22]. The double flash [8] and delayed fluorescence [22] methods are independent of any assumptions about whether the decay of the $P870^+Q_A^-Q_B$ state is direct or proceeds via thermal repopulation of the $P870^+Q_AQ_B^-$ state. The close agreement indicates that the direct process is not quantitatively important in the decay of the $P870^+Q_AQ_B^-$ state [8,14]. A contribution of direct decay of 0.1 s^{-1} affects the apparent equilibrium constant determined using Eqn. 2 so that the calculated free-energy change is reduced by about 5 meV. Since the values using the various methods agree to approximately this amount, we estimate an upper limit of 0.1 s^{-1} for k_{31}, although a value of 0 was used to calculate the thermodynamic data presented in Table I and Fig. 5. The standard-state

enthalpy change found in this work is somewhat smaller than the value of −230 meV found by Kleinfeld et al. [8].

A qualitative potential-energy diagram for the first few steps in the photochemical reaction pathway of bacterial reaction centers is shown in Fig. 6. The ultrafast kinetics and weak temperature dependences of the earliest reactions indicate that the surfaces intersect near the bottom of the potential energy wells. The substantial activation energy of the $P870^+Q_A^-Q_B \rightarrow P870^+Q_AQ_B^-$ reaction suggests that at this point the direct recombination reaction is sufficiently slow due to the increased distance between oxidized and reduced species that an activated step is fast enough at room temperature to maintain high quantum efficiency. Diagrams similar to Fig. 6 have been used by Warshel and coworkers [29,30] to explain efficiency in photosynthetic systems. A combination of a redox-potential gradient and dielectric stabilization of charge-separated states by fixed charges in the interior of the protein provides an efficient and irreversible pathway for energy storage across a membrane.

The substantial negative entropy change upon transfer of an electron from Q_A to Q_B could result from any of several molecular processes. Q_B is the most accessible to the solution of any of the early electron acceptor species, and may organize solvent molecules around it substantially more effectively than Q_A, leading to an entropy decrease. Another possibility is that proton uptake from solution would reduce the number of species present in the system, leading to an entropy decrease. This seems somewhat unlikely to be a major contributing factor, since the overall free-energy change is unchanged at lower pH, while the proton uptake decreases. Determination of the entropy and enthalpy contributions as a function of pH would be useful in determining the magnitude of the effect of proton binding. Finally, an increase in the frequency of one or more molecular vibrations in the reaction center upon electron transfer from Q_A to Q_B would lead to a decrease in the relative population of the vibrating mode(s) and, therefore, an entropy decrease. Resonance Raman experiments on reaction centers in the Q_A^- and Q_B^- states might show if this were indeed the case.

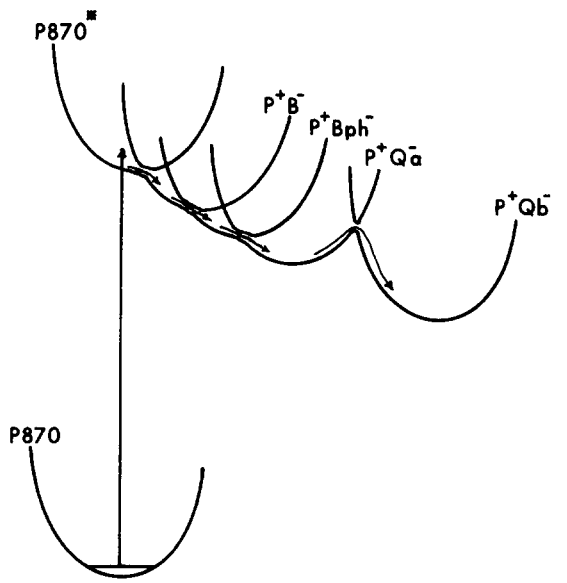

Fig. 6. Potential-energy curve for the early electron transfer reactions in bacterial reaction centers. The various states are identified in the Introduction.

While a thermodynamic analysis of the sort presented in this upper suffices to give a qualitative picture of the potential energy surface for the reaction studied, there certainly is not a one-to-one correspondence between the two quantities. This question has been analyzed recently for cytochrome *c* by Churg et al. [31].

Appendix

An equivalent kinetic scheme for the quinone acceptor system in *Rps. sphaeroides* is shown in Fig. A1. State A_1 is the ground state $P870Q_AQ_B$, A_2 is state $P870^+Q_A^-Q_B$ and A_3 is state $P870^+Q_AQ_B^-$. Acceptors prior to Q_A are incorporated into the light-dependent rate constant k_{12}, which is actually the product of an absorption cross-section and an intensity. The differential equations that describe the behavior of this system are:

$$\frac{d[A_1]}{dt} = -k_{12}[A_1] + k_{21}[A_2] + k_{31}[A_3] \quad \text{(A1a)}$$

$$\frac{d[A_2]}{dt} = k_{12}[A_1] - (k_{23} + k_{21})[A_2] + k_{32}[A_3] \quad \text{(A1b)}$$

$$\frac{d[A_3]}{dt} = k_{23}[A_2] - (k_{31} + k_{32})[A_3] \quad \text{(A1c)}$$

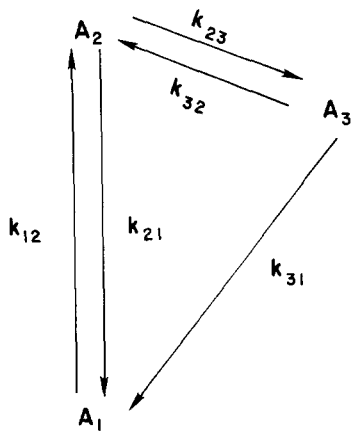

Fig. A1. Equivalent kinetic scheme. State A_1 is $P870Q_AQ_B$, A_2 is $P870^+Q_A^-Q_B$ and A_3 is $P870^+Q_AQ_B^-$.

The solution to this set of equations has the form:

$$A_i(t) = A_i(0)\left(C_{1i} + C_{2i}e^{-\lambda_2 t} + C_{3i}e^{-\lambda_3 t}\right) \quad \text{(A2)}$$

where the A_i's are concentrations of the three species, the C's are amplitude factors, and the λ's are relaxation rate constants for the system. The solution to this set of equations is in most kinetics textbooks, e.g. Ref. 27. The relaxation rate constants are of primary interest, and are given exactly by:

$$\lambda_2 = \tfrac{1}{2}(p+q) \quad \text{(A3a)}$$

$$\lambda_3 = \tfrac{1}{2}(p-q) \quad \text{(A3b)}$$

where

$$p = k_{12} + k_{21} + k_{23} + k_{32} + k_{31} \quad \text{(A4a)}$$

$$q = \left[p^2 - 4(k_{12}k_{23} + k_{12}k_{32} + k_{12}k_{31} + k_{21}k_{32} + k_{21}k_{31} + k_{23}k_{31})\right]^{1/2} \quad \text{(A4b)}$$

Since the approximate values of all the rate constants are known ($k_{23} \approx 5000\ s^{-1}$, $k_{32} \approx 100\ s^{-1}$, $k_{21} \approx 10\ s^{-1}$, $k_{31} \leqslant 1\ s^{-1}$, $k_{12} \leqslant 1\ s^{-1}$), appropriate approximations can be made and the equations simplified considerably. The relation $(1 \pm a)^m \approx 1 \pm ma$ [32] leads to:

$$\lambda_2 = p - \Sigma/p \quad \text{(A5a)}$$

$$\lambda_3 = \Sigma/p \quad \text{(A5b)}$$

where $\Sigma = k_{12}k_{23} + k_{12}k_{32} + k_{12}k_{31} + k_{21}k_{32} + k_{21}k_{31} + k_{23}k_{31}$. If:

$$K = k_{23}/k_{32} \quad \text{(A6)}$$

is the equilibrium constant of the $P870^+Q_A^-Q_B \rightarrow P870^+Q_AQ_B^-$ reaction, then minor terms can be eliminated to give:

$$\lambda_2 = k_{23} + k_{32} \quad \text{(A7a)}$$

$$\lambda_3 = k_{12} + \frac{k_{21}}{K+1} + \frac{k_{31}K}{K+1} \quad \text{(A7b)}$$

Using the typical values of the rate constants quoted above, the approximate values of λ_2 and λ_3 calculated using Eqn. A7 are within 0.2% of the exact values obtained using Eqn. A3.

The dependence of λ_3 on the intensity of measuring light through k_{12} is readily understood if the system is viewed as having been perturbed from equilibrium (actually a photostationary state in this case) by the laser pulse and is relaxing back to the preflash condition. The relaxation-rate constant in such a system is the sum of all relevant rate constants. The quasi-equilibrium between the two charge-separated states is rapidly established with rate constant $\lambda_2 = k_{23} + k_{32}$. The three terms of the eventual approach to steady state described by Eqn. A7b represent effective rate constants for production of the charge-separated states (k_{12}), decay to the ground state via $P870^+Q_A^-$ ($k_{21}/K + 1$) and direct decay to the ground state from $P870^+Q_B^-$ ($k_{31}K/K + 1$). The approximate solutions will not be valid under conditions (e.g., low temperature where the equilibrium between the two charge-separated states is not established rapidly compared to recombination. The mechanism of the $P870^+Q_A^-$ recombination process (direct or via excited states) does not affect the analysis since measured values of k_{21} at each temperature are used in all calculations.

Acknowledgements

This work was supported by grants from the Competitive Research Grants Office of the U.S.

Department of Agriculture (80-CRCR-1-0473), the Herman Frasch Foundation, and a William and Flora Hewlett Foundation Grant of Research Corporation. We thank A. Warshel for stimulating discussions.

References

1 Clayton, R.K. and Sistrom, W.R. (eds.) (1978) The Photosynthetic Bacteria, Plenum, New York
2 Govindjee (ed.) (1982) Photosynthesis: Energy Conversion by Plants and Bacteria, Academic Press, New York
3 Parson, W.W. (1982) Annu. Rev. Biophys. Bioeng. 11, 57–80
4 Rockley, M.G., Windsor, M.W., Cogdell, R.J. and Parson, W.W. (1975) Proc. Natl. Acad. Sci. U.S.A. 72, 2251–2255
5 Kaufmann, K.J., Dutton, P.L., Netzel, T.L., Leigh, J.S. and Rentzepis, P.M. (1975) Science 188, 1301–1304
6 Okamura, M.Y., Isaacson, R.A. and Feher, G. (1975) Proc. Natl. Acad. Sci. U.S.A. 72, 3441–3495
7 Parson, W.W. (1969) Biochim. Biophys. Acta 189, 384–396
8 Kleinfeld, D., Okamura, M.Y. and Feher, G. (1982) Biophys. J. 37, 110a
9 Chamorovsky, S.K., Remennikov, S.M., Kononenko, A.A., Venediktov, P.S. and Rubin, A.B. (1976) Biochim. Biophys. Acta 430, 62–70
10 Vermeglio, A. and Clayton, R.K. (1977) Biochim. Biophys. Acta 461, 159–165
11 Vermeglio, A. (1982) in Function of Quinones in Energy Conserving Systems (Trumpower, B.L., ed.), 169–180, Academic Press, New York
12 Wraight, C.A. (1977) Biochim. Biophys. Acta 459, 525–531
13 Vermeglio, A. (1977) Biochim. Biophys. Acta 459, 516–524
14 Wraight, C.A. (1979) Biochim. Biophys. Acta 548, 309–327
15 Wraight, C.A. (1982) in Function of Quinones in Energy Conserving Systems (Trumpower, B.L., ed.), 181–197, Academic Press, New York
16 Clayton, R.K. and Yau, H.F. (1972) Biophys. J. 12, 867–881
17 Blankenship, R.E. and Parson, W.W. (1979) Biochim. Biophys. Acta 545, 429–444
18 Vermeglio, A., Martinet, T. and Clayton, R.K. (1980) Proc. Natl. Acad. Sci. U.S.A. 77, 1809–1813
19 Wraight, C.A. and Stein, R.R. (1980) FEBS Lett. 113, 73–77
20 Case, G.D. and Parson, W.W. (1971) Biochim. Biophys. Acta 253, 187–202
21 Rutherford, A.W. and Evans, M.C.W. (1980) FEBS Lett. 110, 257–261
22 Arata, H. and Parson, W.W. (1981) Biochim. Biophys. Acta 638, 201–209
23 Good, N.E. and Izawa, S. (1972) Methods Enzymol. 24B, 53–68
24 Cho, H.M., Mancino, L.J. and Blankenship, R.E. (1983) Biophys. J., in the press
25 Bevington, P.R. (1969) Data Reduction and Error Analysis for the Physical Sciences, McGraw-Hill, New York
26 Mortimer, R.G. (1981) Mathematics for Physical Chemistry, Macmillan, New York
27 Moore, J.W. and Pearson, R.G. (1981) Kinetics and Mechanism, 3rd Edn., Wiley, New York
28 Eyring, H., Walter, J. and Kimball, G.E. (1944) Quantum Chemistry, Wiley, New York
29 Warshel, A. and Schlosser, D.W. (1981) Proc. Natl. Acad. Sci. U.S.A. 78, 5564–5568
30 Warshel, A. (1981) Isr. J. Chem. 21, 341–347
31 Churg, A.K., Weiss, R.M., Warshel, A. and Takano, T. (1983) J. Phys. Chem. 87, 1683–1694
32 Weast, R.C. (ed.) (1962) CRC Handbook of Chemistry and Physics, 44th Edn., Chemical Rubber Co., Cleveland, OH